Acetate-catalyzed hydroboration of CO 2 for the selective formation of methanol-equivalent products

Yuri C. A. Sokolovicz, Olalla Nieto Faza, David Specklin, Béatrice Jacques, Carlos Silva López, João dos Santos, Henri Schrekker, Samuel Dagorne

Acetate-catalyzed hydroboration of CO_2 for the selective formation of methanol-equivalent products[†]

Yuri C. A. Sokolovicz[a,b], Olalla Nieto Faza[c], David Specklin[a], Béatrice Jacques[a], Carlos Silva López[c], João H. Z. dos Santos[b], Henri S. Schrekker[b,*], Samuel Dagorne[a,*]

[a]*Institute of Chemistry, Université de Strasbourg, CNRS, Strasbourg, France.*

[b]*Institute of Chemistry, Universidade Federal do Rio Grande do Sul, Porto Alegre, RS, Brazil.*

[c] *Depto. Química Orgánica, Universidade de Vigo, Facultade de Ciencias*

Campus As Lagoas, 32004, Ourense, Spain

[†] Electronic supplementary information (ESI) available: NMR data of compounds, catalytic runs, monitoring experiments. Atom coordinates of all DFT modeled species (xyz files) and molecular structures of transition states.

[*] Email : dagorne@unistra.fr, henri.schrekker@ufrgs.br,

Abstract. The present study details the use of the acetate anion, inexpensive and robust anion, as a CO_2 hydroboration catalyst for the selective formation, in most cases, of methanol-equivalent borane products. Thus, upon heating (90 °C, PhBr), tetrabutylammonium, sodium and potassium acetate (**1**, **2** and **3**, respectively) effectively catalyze CO_2 hydroboration by pinacolborane (pinB–H) to afford CO_2 reduction products HOCOBpin (**A**), pinBOCH$_2$OBpin (**B**) and methoxyborane (**C**). In most cases, a high selectivity in product **C** with higher borane loading and longer reaction time with TONs up to 970. The reduction catalysis remains efficient at low catalyst loading (down to 0.1 mol%) and may also be performed under solvent-free conditions using salt **1** as catalyst, reflecting the excellent robustness and stability of the acetate anion. In control experiments, a 1/1 **1**/pinB–H mixture was found to react fast with CO_2 at room temperature to produce formate species [pinB(O$_2$CH)(OAc)][N(*n*Bu)$_4$] (**5**) through CO_2 insertion into the B–H bond. DFT calculations were also performed to gain insight on the acetate-mediated CO_2 hydroboration catalysis, which further supported the crucial role of acetate as a Lewis base for CO_2 functionalization catalysis by pinB–H. The DFT-estimated mechanism is in line with experimental data and rationalizes the formation of the most thermodynamically stable reduction product **C** through acetate catalysis.

Introduction

The reduction/functionalization of carbon dioxide, a cheap and readily available C1 source, is currently attracting considerable interest to access valuable chemicals, most notably methanol.[1,2] However, the high thermodynamic stability of CO_2 requires the development of effective catalysts for CO_2 activation and functionalization catalysis. To this end, numerous metal-based homogeneous catalysts have been investigated over the past years using hydrogen,[3] hydroboranes[4] and hydrosilanes[5] as reducting agents. While direct CO_2 reductive hydrogenation with H_2 is most desired for atom economy, only a few discrete metal catalysts, mostly based expensive noble metal sources, may efficiently catalyze such a transformation given the relative inertness of H_2.[3,3,6] Thus, the use of reductants such as hydroboranes and hydrosilanes, which are more reactive due to a polar H–E bond (E = B, Si), has led to significant developments in metal-catalyzed CO_2 reductions, including a number of product-selective catalytic systems (at the formate, ketal, methanol and methane reduction level) with transition as well as main group metal centers.[4,5,7] In contrast, metal-free catalysts for CO_2 hydro-boration/-silylation remain far less studied since the first report by Fontaine using an ambiphilic phosphino-borane species as a highly active CO_2 hydroboration catalyst.[8] In the area, additional ambiphilic as well as Frustrated Lewis pairs (FLP) systems of the type P/B and N/silylium,[9] have been reported be effective in CO_2 hydroboration catalysis. Also, as first shown by Cantat,[10] strong organic Lewis bases may also catalytically hydroborate CO_2. The latter approach was successfully implemented with strong Lewis bases such as guanidines,[10a] phosphines,[9b] proton sponge,[11] zwitterionic carbenoids/diazafluorenides,[12] abnormal *N*-heterocyclic carbenes[13] and carbodiimides[14]. Since most strong bases are air- or/and moisture-sensitive, further progress in the area may involve the development of highly robust, air-stable and cheap Lewis bases for CO_2 hydroboration. To this end, we have become interested into investigating the acetate anion for use in CO_2 hydroboration catalysis. Though acetate is a

weak Lewis base, acetate salts are particularly attractive for use in catalysis since they are extremely stable, available on a large scale, inexpensive, benign and have thus found widespread applications ranging from use as deicing agents, food additives to catalysts in polymer industry.[15]

Using simple sodium, potassium and tetrabutylammonium acetate salts, we here report the acetate-catalyzed reduction of CO_2 by hydroboranes for the selective production of the methanol-equivalent product. In addition to catalysis results, combined experimental and computational studies were also performed to provide insight into the hydroboration mechanism, the results of which are also discussed herein.

Results-Discussion

Tetrabutylammonium, sodium and potassium acetate salts (**1**, **2** and **3**, respectively) were tested as catalysts in the hydroboration of CO_2 using pinacol borane (H–Bpin) as a borane source. The results are compiled in Table 1 and all associated experimental dataare included in the ESI.

Table 1. Acetate-catalyzed reduction of CO_2 with pinB–H.[a]

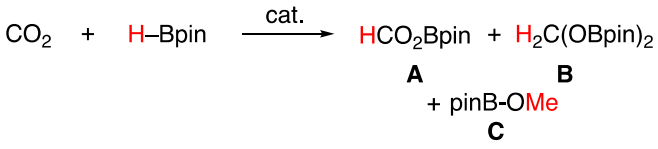

Entry	Cat.	Solvent	T (°C)	t (h)	Conv.[b] (%)	Selectivity (%) [c] in A	B	C	TON[d]
1[e]	**1** (5 mol %)	C_6D_6	90	2	62	100	-	-	12.4
2[e]	**1** (5 mol %)	C_6D_6	90	26	82	66	7	27	16.4
3	**1** (5 mol %)	C_6D_6	90	26	99	0	0	100	20
4	**1** (0.5 mol %)	C_6D_6	90	2	40	2	3	95	80
5	**1** (0.5 mol %)	C_6D_6	90	20	96	1	< 1	98	192
6	**1** (0.1 mol %)	C_6D_6	90	46	94	1	0	99	940

7	**1** (0.1 mol %)	Solvent -free	90	19	97	0	0	100	970
8	**2** (0.1 mol%)	C_6D_5Br	120	48	88	1	0	99	880
9	**2** (0.1 mol%)	C_6D_5Br	120	65	96	1	0	99	960
10	**3** (0.1 mol%)	C_6D_5Br	120	65	85	1	0	99	850
11	**3** (0.1 mol%)	C_6D_5Br	120	65	94	1	0	99	940

[a] Conditions (unless indicated otherwise): $[pinB–H]_0$ = 3 M, $P_0(CO_2)$ = 1.5 atm, C_6D_6 or C_6D_5Br (0.5 mL). [b] Conv. = borane conversion to **A**, **B** and **C**, as estimated from ^1H and ^{11}B NMR data (C_6Me_6 was used as an internal standard). [c] the relative amount of reduction products HOCOBpin (**A**), $pinBOCH_2OBpin$ (**B**) and methoxyborane (**C**) was estimated from ^1H and ^{11}B NMR data. [d] TON = Turnover number (based on borane consumption). [e] Conditions: $[pinB–H]_0$ = 0.3 M, $P_0(CO_2)$ = 1.5 atm, C_6D_6 (0.5 mL).

The ammonium salt **1** was first screened as catalyst due to its better solubility in common organic solvents compared to inorganic salts **2** and **3**. Satisfyingly, in an initial test, species **1** (5 mol%) was found to catalyze CO_2 hydroboration by pinB–H (90 °C, C_6D_6, 1.5 atm CO_2) to selectively afford the mono-reduction product $pinB–CO_2H$ (**A**) after 2h of reaction, with a 62% conversion of pinB–H (entry 1, Table 1), thereby showing the ability of the acetate ion to effectively catalyze CO_2 reduction. In such reaction conditions, longer reaction times led to higher borane conversion (as estimated from ^{11}B and ^1H data) along with the formation of double- and triple-reduction products $pinB–O–CH_2–O–Bpin$ (**B**) and pinB–OMe (**C**). Thus, a 82% borane conversion to a 66/7/27 **A**/**B**/**C** mixture (along with pinB–O–Bpin as a side-product) was observed after 26h, as deduced from ^1H and ^{11}B NMR monitoring data and comparison with literature data (entry 2, Table 1).[16] In particular, the ^1H NMR spectrum of the crude mixture contains singlet resonances at δ 8.12, 5.27 and 3.50 ppm assigned to the HCO_2-Bpin, $pinB–O–CH_2–O–Bpin$ and pinB–O*Me* moieties, respectively. The ^{11}B NMR spectrum features a characteristic broad signal (δ 22.9 ppm) assigned to **A**, **B** and **C**. In line with previous reports on CO_2 hydroboration catalysis, the formation of **C** (from **B** and H–Bpin) comes along with the production of side-product pinB–O–Bpin, as evidenced

by ^{11}B NMR (br, δ = 21.8 ppm; ESI). Under identical reaction conditions but using a ten-fold increase in borane loading (entry 3, Table 1), the selective and quantitative formation methoxyborane product **C** was observed after 26 h (90 °C, C_6D_6).[17] This clearly indicates that the lower selectivity in the initial run (formation of **A**, **B** and **C)** is due to the lower loading in pinB–H, which thus decreases the reaction rate and limits the extent of the reduction. Remarkably, acetate-catalyzed CO_2 reduction is also highly effective at much lower acetate amounts, such as 0.5 and 0.1 mol% in **1** (entries 4-6, table 1) with the nearly quantitative production of methanol-equivalent **C** after 20 and 46 h, respectively. Again, the large excess in borane *vs.* CO_2 under such low acetate loadings certainly promote the formation of the triple-reduction CO_2 reduced product, thus the high selectivity in **C**. It is also noteworthy that CO_2 reduction may be performed under solvent-free conditions (with H–Bpin acting as solvent and reagent) to further boost catalytic activity. Thus, a 1000/1 H–Bpin/**1** mixture heated at 90 °C for 19h under CO_2 (1.5 atm) performed best with the nearly quantitative formation of reduction product **C** (entry 7, Table 1; TON = 970), reflecting the excellent stability and robustness catalyst **1** under such reaction conditions.[18]

Unlike ammonium salt **1**, inorganic salts NaOAc (**2**) and KOAc (**3**) are inactive CO_2 reduction in the presence of H–Bpin at 90 °C in benzene or PhBr due to their poor solubility under these conditions. However, salt **2** and **3** at 0.1 mol% loading (*vs.* H–Bpin) both catalyze CO_2 hydroboration at higher temperature (PhBr, 120 °C, 1.5 atm CO_2) to selectively afford methoxyborane **C** (along with pinB–O–Bpin) in good to nearly quantitative conversion, (entries 7-10, Table 1). The higher reaction temperature (120 ºC for **2** and **3** *vs.* 90 °C for **1**), required for the solubilization of inorganic salts **2** and **3**, is thus not detrimental to catalyst selectivity and overall effectiveness (TONs: 960 and 940 h^{-1}), though longer reaction times were necessary for high conversion.

Acetate salts **1**-**3** were also tested in CO_2 reduction catalysis using H_3B-SMe_2 (BMS),

a cheap hydroborane source since readily available from industrially produced B_2H_6. The results are compiled in Table 2.

Table 2. Acetate-catalyzed reduction of CO_2 with BH_3-SMe_2.[a]

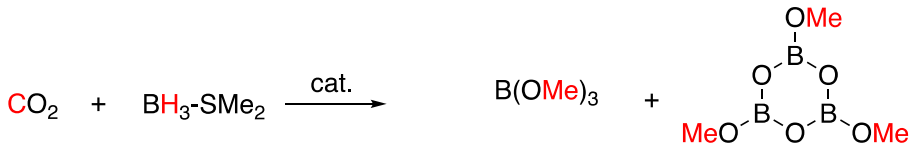

D **E**

Entry	Cat.	Solvent	T (°C)	t (h)	Conv.[b] (%)	Selectivity (%)[c] D	E	TON[d]
1[e]	**1** (10 mol %)	C_6D_6	RT	17	100	30	70	10
2	**1** (10 mol %)	C_6D_6	RT	17	100	0	100	10
3	**1** (1 mol %)	C_6D_6	RT	48	68	0	100	68
4	**1** (1 mol %)	C_6D_6	60	20	96	0	100	96
5	**1** (0.1 mol %)	C_6D_6	60	20	75	0	100	750

[a] Conditions (unless indicated otherwise): $[Me_2S\text{-}BH_3]_0$ = 3.3 M, $P_0(CO_2)$ = 1.5 atm, C_6D_6 or C_6D_5Br (0.5 mL). [b] Conv. = borane conversion, as estimated from ^1H and ^{11}B NMR data. [c] the relative amount of reduction products **D** and **E** was estimated from ^1H and ^{11}B NMR data. [d] TON = Turnover number, based on borane consumption (C_6Me_6 was used as an internal standard). [e] Conditions: $[Me_2S\text{-}BH_3]_0$ = 0.33 M, $P_0(CO_2)$ = 1.5 atm, C_6D_6 (0.5 mL).

Satisfyingly, ammonium salt **1** (10 mol%) catalyzes CO_2 hydroboration at room temperature in the presence of BMS to quantitatively afford after 17h a 70/30 mixture of trimethoxyboroxine (**E**) and $B(OMe)_3$ (**D**), as estimated from ^1H and ^{11}B data and comparison with literature data (entry 1, Table 2).[8a,19] In particular, the ^1H spectrum of the crude mixture contains characteristic singlet resonances at δ 3.35 and 3.44 ppm (in a 66/34 ratio), attributed to the O*Me* moieties of products **E** and **D**, respectively (see ESI). ^{11}B NMR data clearly indicated the complete consumption of BMS along the formation **D** and **E** (δ 18.7 and 19.1 ppm, respectively; ESI).[19] Using a ten-fold increase in the BMS feed (while keeping a 10%

catalyst loading; entry 2, Table 1) led to the quantitative formation of reduction product **E** after 17 h at RT, indicating that BMS was a rate-limiting reagent in the initial run. With a lower catalyst loading (1 mol% of catalyst **1**), the selective formation of **E** was also observed at room temperature, yet with only 68% BMS consumption to **E** after 48 h (entry 3, Table 2). Quantitative CO_2 reduction to boroxine **E** was however achieved at 60 °C using 1 mol % of catalyst **1** (entry 4, Table 2). CO_2 reduction catalysis also proceeds using 0.1 mol% of **1** (*vs*. BMS) to produce **E** (75% BMS consumption after 20h; entry 5, Table 2), further establishing **1** as an effective CO_2 reduction catalyst by BMS to methanol-equivalent products (TON up to 750). In contrast, no CO_2 reduction (by BMS) activity was observed using inorganic salts **2** and **3** at room temperature due to the poor solubility of those salts, while higher reaction temperatures (from 40 to 80 °C) only led to unidentified decomposition products. Overall, the above results establish the acetate ion, a weak Lewis base, as a robust and effective CO_2 hydroboration catalyst using either pinB–H or BMS as a hydroborane source.

Stoichiometric control experiments on the 1/pinB–H/CO_2 system. To better understand the acetate-catalyzed CO_2 hydroboration and the role of the acetate ion, NMR-scale control reactions with the **1**/pinB–H/CO_2 system were carried out and monitored by ^{1}H and ^{11}B NMR (Figure 1). ^{1}H and ^{11}B NMR data recorded after the addition of **1** to 1 equiv of pinB–H (RT, C_6D_6, 15min) suggests the labile coordination of the acetate ion to pinB–H, with a fast acetate coordination/decoordination on the NMR timescale under the studied conditions.[20] However, an adduct of the type $[pinB(H)(OAc)]^-$ could not be completely characterized.[21] While no reaction was observed between pinB–H and CO_2 (1.5 atm) after 24 h at RT in C_6D_6, the 1/1 **1**/pinB–H mixture reacts fast with CO_2 at room temperature (1.5 atm CO_2, C_6D_6, 15min) to quantitatively afford the formate insertion product $pinB(CO_2H)(OAc)^-$ (**4**, Figure 1), which results from CO_2 insertion into the B–H bond. This clearly reflects a more nucleophilic pinB–*H* hydride, further suggesting acetate coordination to pinB–H. The

identity of species **4** is proposed on the basis of ^{1}H, ^{13}C, ^{11}B NMR and 2D (HSQC and HMBC) NMR data, which all support the presence of a formate group connected to a four-coordinate B(III) center. For instance, the ^{1}H and ^{13}C NMR data of the reaction of **4** with CO_2 contains characteristic HCO_2 (δ 9.18 ppm) and HCO_2 (δ 66.0 ppm) resonances for a formate moiety, while the ^{11}B NMR spectrum, with a singlet signal at δ = 8.35 ppm, agrees with a four-coordinated B(III) center. Though species **4** could not be isolated in a pure form, its *in situ* formation rationalizes the observed acetate-promoted CO_2 functionalization. Thus, as supported by DFT studies (*vide infra*), species **4** is presumably a key initial intermediate permitting CO_2 hydroboration catalysis with pinB–H.

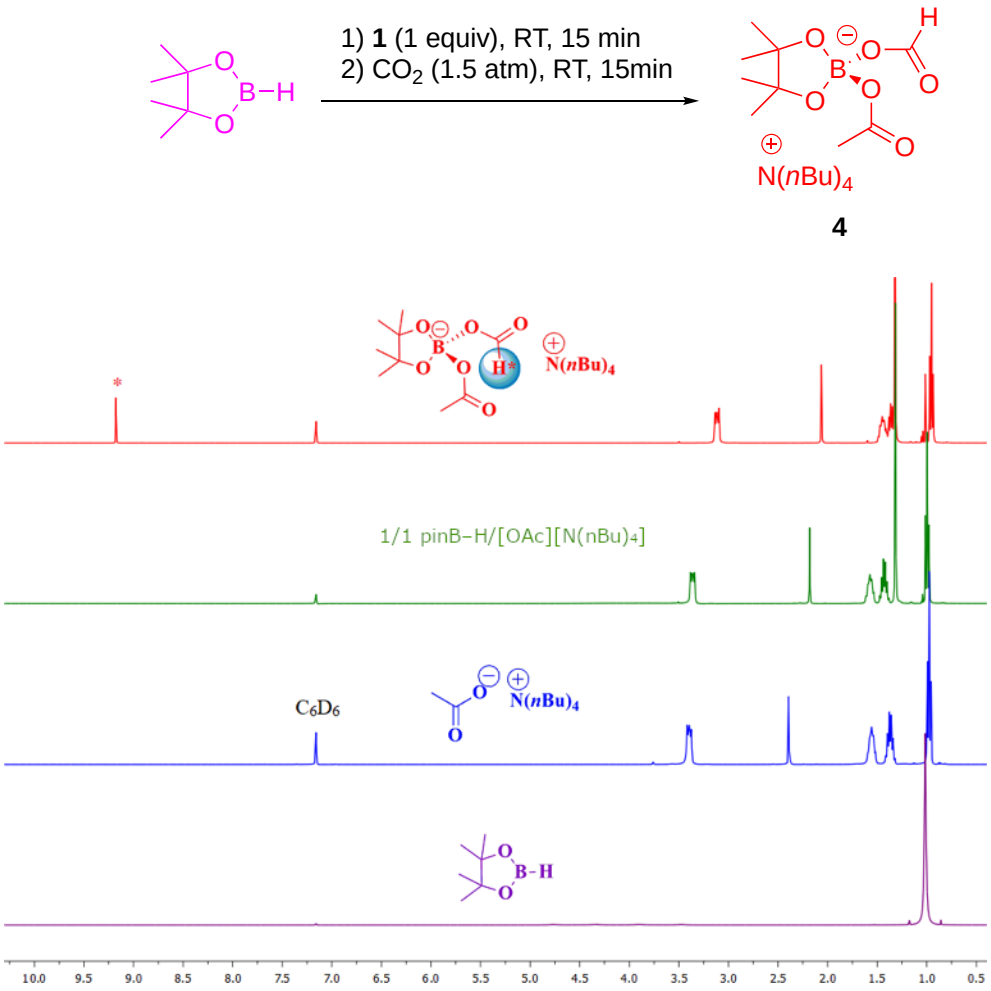

Figure 1. Reaction scheme for the formation of borate species **4** and the corresponding ^{1}H NMR spectra (C_6D_6) of HBpin, **1**, the 1/1 HBpin/**1** mixture and species **4**.

DFT-estimated mechanism. To gain additional insight on and further rationalize the acetate-catalyzed CO_2 hydroboration by pinB–H, mechanistic pathways were computed by DFT at the wB97xD/def2tzvpp//B3LYP/6-31G* theory level. The DFT-derived proposed mechanism is depicted in Figure 2 and the associated molecular structures are included in the ESI. First, combining pinB–H with the acetate ion affords the corresponding borohydride Lewis adduct **OAc-Ad**, through an exergonic reaction (ΔG = -5.6 kcal.mol^{-1}), in line with experimental indications. The reaction of borohydride **OAc-Ad** with CO_2 is then rather facile (energy barrier, $\Delta\Delta G$ = 16.5 kcal.mol^{-1}) to yield the thermodynamically favored formate insertion product **IV** (ΔG = -21.3 kcal.mol^{-1}). The reaction proceeds through an early transition state **TS-1** (ΔG = 10.9 kcal.mol^{-1}) featuring an elongated B–H bond (1.323 vs. 1.229 Å in pinB–H) and a short B–*H*/*C*O_2 distance (1.551 Å). Under catalytic reaction conditions (*i.e.* excess of pinB–H), **IV** may also act as a Lewis base and coordinate a pinB–H unit to provide, through a low barrier process ($\Delta\Delta G$ = 10.4 kcal.mol^{-1}), dinuclear Lewis adduct **V** (ΔG = -12.0 kcal.mol^{-1}), in which the two boron centers are linked by a formate bridge.[22] The formation of model **V** is an endergonic process ($\Delta\Delta G$ = 9.3 kcal.mol^{-1}) from **IV** and pinB-H) and **V** appears to be a central intermediate in the present catalysis. It thus may evolve through two pathways, altogether rationalizating the formation of reduction products **A**, **B** and **C**. The first pathway involves the exergonic reduction of a second CO_2 molecule by the B–H moiety in **V** leading to diboron diformate **VI** (ΔG = -24.7 kcal.mol^{-1}) through a moderate barrier (**TS-3**, $\Delta G^{\ddagger}$ = 11.5 kcal.mol^{-1}; $\Delta\Delta G$ = 23.5 kcal.mol^{-1}). **VI** may then dissociate *via* a low barrier (**TS-4**, $\Delta G^{\ddagger}$ = -18.6 kcal.mol^{-1}) to mono-reduction product pinBO_2CH (**A'**, model of experimentally observed **A**) and re-generate species **IV**. From that point, it should be noted that further reduction of **A'** by reaction with pinB–H to produce **B'** (model of species **B**) was DFT-estimated to proceed *via* a high energy barrier (42.6 kcal/mol), which is not compatible with the reaction conditions. The second pathway from intermediate

V initially proceeds with an intramolecular reduction of the B-OCHO-B bridging formate by the terminal B–H moiety to yield the corresponding ketal product **VII** (ΔG = -24.1 kcal.mol^{-1}). The reaction occurs through four-center transition state **TS-5** ($\Delta G^{\ddagger}$ = 14.2 kcal.mol^{-1}), an exergonic reaction with an energy barrier (26.2 kcal.mol^{-1}) compatible with reaction conditions. Acetate decoordination from **VII** may produce the second-reduction product **B'** given the similar stability of **VII** and **B'** ($\Delta\Delta G$ = -1.1 kcal.mol^{-1}). For the formation of methanol-equivalent **C'**, direct reaction of **B'** with pinB–H was first DFT-estimated, yet leading to **C'** through a prohibitively high energy barrier (63.2 kcal/mol). Rather, both **B'** and acetate adduct **VII** react similarly to undergo an intramolecular reaction through a concerted asynchronous four-center transition state (**TS-6** and **TS-7**, respectively) producing formaldehyde and boroxide pinB–O–Bpin **VIII** (ΔG = -26.9 kcal.mol^{-1}, experimentally observed) from **B'**, and formaldehyde and acetate adduct **IX** (ΔG = -31.9 kcal.mol^{-1}) from **VII**. Here again, acetate coordination favors the reaction as reflected by the substantially lower energy barrier for formaldehyde formation from acetate adduct **VII** *vs.* **B'** ($\Delta\Delta G$ = 25.1 and 37.0 kcal.mol^{-1}, respectively) due to the lower energy of **TS-7** vs. **TS-6**. The acetate pathway is thus clearly favored. Comparing the molecular structures of **TS-7** and **TS-6** shows that acetate coordination significantly lengthens the adjacent B–OCH_2 bond, in line with a more nucleophilic B-*O*CH_2 oxygen upon Lewis adduct formation, which in turn allows B–O–B bond formation at a lower energy cost along with formaldehyde formation. The comparable stability of **VIII** and adduct **IX** suggests that both species are accessible through acetate de-coordination/coordination under the reaction conditions. Then, formaldehyde may subsequently be reduced in the presence of pinB–H and borohydride **OAc-Ad** to produce final reduction product pinB–OMe **C'** (model of **C**, experimentally observed) and re-generating borohydride **OAc-Ad** through a highly exergonic reaction (ΔG = -62.6 kcal.mol^{-1}). The reaction proceeds with a reasonable activation barrier ($\Delta\Delta G$ = 21.1 kcal.mol^{-1}) though the

associated transition state **TS-8** ($\Delta G^{\ddagger}$ = -10.6 kcal.mol^{-1}) is surprisingly low for such an entropically disfavored process. The structure of **TS-8** indicates that pinB–H and **OAc-Ad** reduce formaldehyde in cooperative manner, where pinB–H may act as a Lewis acid for H_2C=O activation and **OAc-Ad** as a hydride source.

Altogether, the proposed DFT mechanism for CO_2 hydroboration is consistent with all experimental and reaction conditions as well as product formation/selectivity (in **A**, **B'** and **C'**). In particular, it may highlighted that: i) the formation of the most thermodynamically stable final model product pinB–OMe (**C'**) certainly drives the reaction to completion explaining the experimentally observed high selectivity in **C** with longer reaction time and higher borane loading; ii) the experimental energy barrier of the overall reaction (35.5 kcal.mol^{-1}, estimated from the difference between the highest energy entity, *i.e.* **TS-5**, and the most stable and observable intermediate, *i.e.* **OAc-Ad**) is in line with the rather harsch reaction conditions; iii) the rate limiting step of the overall reaction (through **TS-5**) is thus the formation of the second reduction product **B'** then readily reduced to **C'**, consistent with experimental data (at most, trace amount of reduction product **B** are observed at the end of the reaction).

Summary – Conclusion

The present study shows that the acetate ion, a weak Lewis base, may effectively catalyze CO_2 hydroboration to methanol-equivalent products using pinB–H and BH_3-SMe_2 as hydroboranes (TON up to 970). Taking advantage of the robustness and stability of such a common and robust anion, the catalysis may be efficiently performed with a low catalyst loading (down to 0.1 mol%) and, in some cases, under solvent-free conditions without any loss in catalytic activity. Combined experimental and DFT calculations data provided mechanistic insights on the CO_2 hydroboration catalysis by pinB–H, showing the key role of

acetate interaction with pinB–H for CO_2 functionalization and subsequent catalysis to occur.

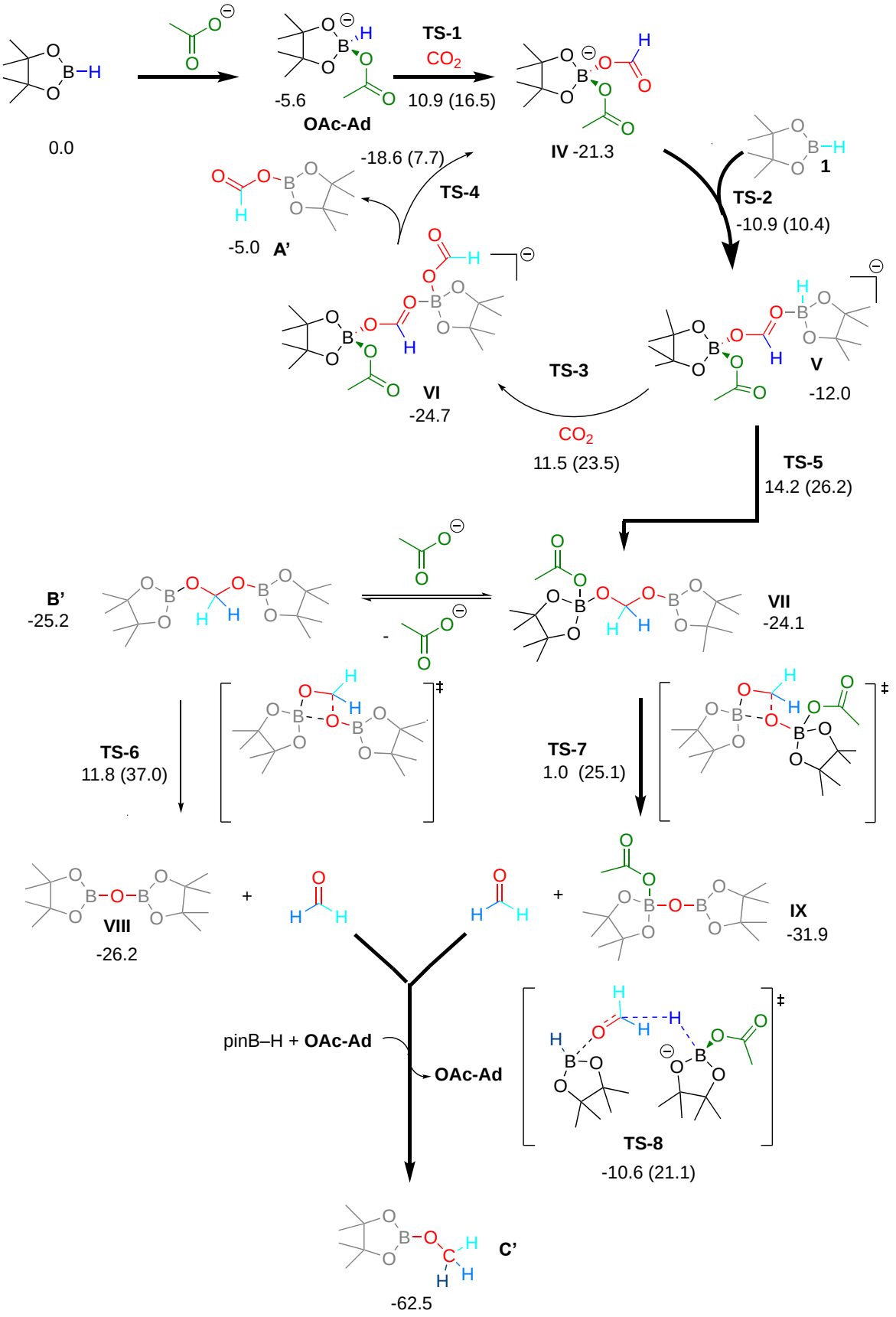

Figure 2. DFT-estimated mechanism (wB97xD/def2tzvpp//B3LYP/6-31G*, benzene) of acetate-catalyzed CO_2 hydroboration and the associated Gibbs free energies. The values in parenthesis correspond to the energy barriers.

Experimental Section

General considerations

Pinacolborane (HBpin), C_6D_6 and C_6D_6Br were purchased from Aldrich and stored over molecular sieves (4 Å) for at least 20 h. Borane dimethyl sulfide was purchased from Strem Chemicals and stored over molecular sieves (4 Å) for at least 20 h. Sodium acetate (**2**) and potassium acetate (**3**) were purchased from Aldrich and dried at 100 ºC under high vacuum for 24 h prior to use. Methanol was distilled over KOH and stored over activated molecular sieves (4 Å) for at least 48 h. 1D and 2D NMR spectra were recorded before and after the CO_2 injection, using Bruker AC 300 MHz, 400 MHz, 500 MHz and 600 MHz NMR spectrometers. NMR chemical shift values were determined relative to the residual protons in C_6D_6 and C_6D_5Br as internal reference for ^1H (δ of the most downfield signal = 7.16, 7.30, 5.32, 7.26 ppm) and $^{13}C\{^1H\}$ (δ of the most downfield signal = 128.39, 130.89, 53.84, 77.23 ppm).

All DFT calculations have been performed with the Gaussian 09 suite of programs, at the wB97xD/def2tzvpp//B3LYP/6-31G* level for the optimization and characterization of all stationary points. The effect of solvent has been included both in geometry optimizations and energy refinement using the integral equation formalism variant of PCM (IEFPCM) with the solvent parameters corresponding to benzene. Harmonic analysis has been carried out at all stationary points, in order to characterize them either as minima or transition states in the potential energy surface, and the stability of the wavefunction has also been checked, to ensure that it is a minimum in the corresponding functional space. For the sake of simplicity, we have not included in our calculations the cationic counterion in the anionic structures.

[N(^{n}Bu)$_4$][OAc] (1). Tetrabutylammonium acetate [N(^{n}Bu)$_4$][OAc] (**1**) was synthesized on a gram-scale *via* a salt metathesis reaction between a stoichiometric amount of potassium acetate and tetrabutylammonium chloride in dry methanol as solvent. Salt **1** was isolated in quantitative yield as a colorless solid. ^{1}H NMR (400 MHz, C_6D_6): δ 3.40 (m, 8H, ^{n}Bu), 2.39 (s, OAc), 1.55 (m, 8H, ^{n}Bu), 1.39-1.34 (m, 8H, ^{n}Bu), 0.97 (t, 8H, ^{n}Bu). ^{13}C NMR (100 MHz, C_6D_6): δ 174.1 (*C*=O), 58.7 (Me-Ac), 24.7 (^{n}Bu), 24.6 (^{n}Bu), 20.3 (^{n}Bu), 14.1 (^{n}Bu).

General procedure for the catalytic reduction of CO_2 by hydroboration with acetate salts 1-3. The catalytic hydroboration of CO_2 was divided in two steps. First, in a dry box, a NMR J. Young tube was charged with the acetate catalyst (**1-3**). In the case of 5 and 10% mol. catalyst loadings, pure catalyst **1-3** was directly added to the NMR tube. In the case of 0.1, 0.5 and 1% mol. catalyst loadings, the appropriate volume of a pre-prepared 1 M solution of catalyst **1-3** (in THF) was added to the NMR tube (THF was then removed *in vacuo* for a couple of hours). C_6D_6 (0.5 mL) and the appropriate amount of borane were subsequently added to the tube along with C_6Me_6 (internal standard). Outside the dry box, the tube was cooled with liquid N_2, the tube was freezed-pumped-thawed, then pressurized with 1.5 bar of CO_2 and allowed to warm to room temperature. The tube was then placed into an oil bath, pre-heated at the desired reaction temperature. The reaction was monitored by ^{1}H and ^{11}B NMR and products assignment was based on literature data.

Hydroboration of CO_2 by pinB–H catalysed by 1 (0.5 mol%) with $[pinBH]_0$ = 3 M. Catalyst **1** (7.46 μmol, 1.0 equiv), HBpin (212 mg, 1.49 mmol, 200 equiv), and hexamethylbenzene (4 mg, 24.6 μmol, 1.5 equiv) as an internal standard in C_6D_6 (0.5 mL) were transferred to a NMR J Young tube. After CO_2 pressurization under 1.5 atm, the tube was heated at 90 ºC and the reaction monitored by ^{1}H and ^{11}B NMR. The ^{1}H and ^{11}B NMR

spectra showed the consumption of 96 % of HBpin to form CH_3OBpin after 20 h. The Turnover number (TON), *i.e.* borane conversion to **A**, **B** and **C**, was calculated by the integration of the ^1H NMR signals of product **A** (*H*OCOBpin, δ = 8.23 ppm) and methoxyborane **C** (MeO-Bpin, δ = 3.44 ppm), using the hexamethylbenzene signal (δ = 2.06 ppm) as reference. After 20 h, the reaction achieved more than 98% of selectivity in **C**. The formation of **A** and **C** was further evidenced and quantified by ^{11}B NMR spectroscopy in accordance with literature data.

Generation of [pinB(O_2CH)(OAc)][N^{n}Bu$_4$] (4). Under a nitrogen atmosphere, a C_6D_6 solution (0.5 mL) containing salt **1** (15 mg, 49.75 µmol) and pinB–H (6.37 mg, 49.75 µmol) was transferred to a NMR J. Young tube. ^1H and ^{11}B NMR spectra were immediately recorded suggesting a labile interaction between the OAc^- anion and pinB–H. The NMR tube was then charged with 1.5 bar of CO_2 at room temperature. The resulting mixture was immediately analyzed by ^1H, ^{13}C, HSQC and HMBC spectroscopy showing showing the complete conversion latter which also showed being unstable when isolated. ^1H NMR (300 MHz, C_6D_6) δ 9.18 (s, HCOO, 1H), 3.27 – 2.88 (m, CH_2, 2H), 2.06 (s, CH_3, 3H), 1.52 – 1.40 (m, CH_2, 2H), 1.40 – 1.34 (m, CH_2, 2H), 1.32 (s, CH_3, 3H), 0.95 (t, CH_3, 3H). ^{11}B NMR (128 MHz, C_6D_6, δ): 8.35 (s, B). ^{13}C NMR (101 MHz, C_6D_6, δ): 171.40 ($OCOCH_3$), 165.97 (OCOH), 79.64 (C_{tert}), 58.53 (CH_2), 25.97 (CH_3), 24.61 (CH_3COO), 24.21 (CH_2), 20.1 (CH_2), 13.95 (CH_3).

Conflicts of interest

There are no conflicts to declare

Acknowledgments. The CNRS (Paris, France) and the University of Strasbourg are acknowledged for financial support. The Brazilian agency Conselho Nacional de Desenvolvimento Científico e Tecnológico (CNPq; Science without Borders Special Visiting Scientist project 405784/2013-9) is acknowledged for financial support. J. H. Z. S., and H. S. S. are grateful to CNPq for the PQ fellowships. Jordan Parmentier (University of Strasbourg) is acknowledged for low temperature 1D and 2D NMR experiments and additional blank catalytic runs.

References

1. (a) *Catalysis for Sustainability: Goals, Challenges and Impacts*, Ed.: T. P. Umile, CRC Press, Taylor and Francis, 2016. (b) M. Aresta, *Carbon dioxide as Chemical Feedstock*, Wiley-VCH Verlag GmbH & Co. KGaA, 2010.

2. G. A. Olah, A. Goeppert and G. K. S. Prakash, *Beyond Oil and Gas: The Methanol Economy*, Wiley-VCH Verlag GmbH & Co. KGaA, 2009.

3. (a) W.-H. Wang, Y. Himeda, J. T. Muckerman, G. F. Manbeck and E. Fujita, *Chem. Rev.*, 2015, **115**, 12936–12973. (b) T. Zell and D. Milstein, *Acc. Chem. Res.*, 2015, **48**, 1979–1994.

4. (a) S. Bontemps, *Coord. Chem. Rev.*, 2016, **308**, 117–130. (b) S. Chakraborty, P. Bhattacharya, H. Dai and H. Guan, *Acc. Chem. Res.*, 2015, **48**, 1995–2003. (c) C. C. Chong and R. Kinjo, *ACS Catal.* 2015, **5**, 3238; (c) L. Zhang and Z. Hou, *Chem. Sci.* 2013, **4**, 3395–3403.

5. (a) F. J. Fernández- Alvarez and L. A. Oro, *ChemCatChem*, 2018, **10**, 4783–4796. (b) A. Tlili, E. Blondiaux, X. Frogneux and T. Cantat, *Green Chem.*, 2015, **17**, 157–168; e) F. J. Fernández-Alvarez, A. M. Aitani and L. A. Oro, *Catal. Sci. Technol.*, 2014, **4**, 611–624.

6. (a) W. H. Wang, J. F. Hull, J. T. Muckerman, E. Fujita and Y. Himeda, *Energy Environ. Sci.*, 2012, **5**, 7923–7926. (b) R. Tanaka, M. Yamashita and K. Nozaki, *J. Am. Chem. Soc.*, 2009, **131**, 14168–14169. (c) X.-L. Du, Z. Jiang, D. S. Su and J.-Q. Wang, *ChemSusChem*,

2016, **9**, 322–332. (d) W. H. Bernskoetter and N. Hazari, *Acc. Chem. Res.*, 2017, **50**, 1049–1058;

7. Recent representative examples with main group metal catalysts: (a) A. Caise, D. Jones, E. L. Kolychev, J. Hicks, J. M. Goicoechea and S. Aldridge, *Chem. Eur. J.*, 2018, **24**, 13624–13635. (b) J. A. B. Abdalla, I. M. Riddlestone, R. Tirfoin and S. Aldridge, *Angew. Chem. Int. Ed.* 2015, **54**, 5098–5102. (c) D. Specklin, F. Hild, C. Fliedel, C. Gourlaouen, L. F. Veiros and S. Dagorne, *Chem. Eur. J.*, 2017, **23**, 15908–15912. (d) S. Dagorne and R. Wehmschulte, *ChemCatChem*, 2018, **10**, 2509–2520.

8. (a) M.-A. Courtemanche, M.-A. Légaré, L. Maron and F.-G. Fontaine, *J. Am. Chem. Soc.*, 2013, **135**, 9326–9329. (b) F.-G. Fontaine and É. Rochette, *Acc. Chem. Res.*, 2018, **51**, 454–464. (c) R. Declercq, G. Bouhadir, D. Bourissou, M.-A. Légaré, M.-A. Courtemanche, K. S. Nahi, N. Bouchard, F.-G. Fontaine and L. Maron, *ACS Catal.*, 2015, **5**, 2513–2520.

9. For instance, see: (a) F.-G. Fontaine, M.-A. Courtemanche, M.-A. Légaré and É. Rochette, *Coord. Chem. Rev.*, 2017, **334**, 124–135. (b) T. Wang, D. W. Stephan, *Chem. Commun.*, 2014, **50**, 7007–7010. (c) N. von Wolff, G. Lefèvre, J.-C. Berthet, P. Thuéry, T. Cantat, *ACS Catal.* 2016, **6**, 4526–4535.

10. (a) C. Das Neves Gomes, E. Blondiaux, P. Thuéry and T. Cantat, *Chem. Eur. J.*, 2014, **20**, 7098–7106. (b) E. Blondiaux, J. Pouessel and T. Cantat, *Angew. Chem. Int. Ed.*, 2014, **53**, 12186–12190.

11. M.-A. Légaré, M.-A. Courtemanche and F.-G. Fontaine, *Chem. Commun.*, 2014, **50**, 11362–11365.

12. Y. Yang, M. Xu and D. Song, *Chem. Commun.*, 2015, **51**, 11293–11296.

13. (a) S. C. Sau, R. Bhattacharjee, P. K. Vardhanapu, G. Vijaykumar, A. Datta and S. K. Mandal, *Angew. Chem. Int. Ed.*, 2016, **55**, 15147–15151. (b) S. Chandra Sau, R. Bhattacharjee, P. K. Hota, P. K. Vardhanapu, G. Vijaykumar, R. Govindarajan, A. Datta and S. K. Mandal, *Chem. Sci.*, 2019, **10**, 1879–1884.

14 (a) A. Ramos, A. Antiñolo, F. Carrillo-Hermosilla, R. Fernández-Galán, A. Rodríguez-Diéguez and D.García-Vivó, *Chem. Commun.*, 2018, **54**, 4700–4703.

15. C. Le Berre, P. Serp, P. Kalck and G. P. Torrence, Ullmann's Encyclopedia of Industrial Chemistry, 2014, 1–34.

16. S. Bontemps, L. Vendier and S. Sabo-Etienne, *Angew. Chem. Int. Ed.*, 2012, **51**, 1671–1674.

17. A blank test run under such conditions (with only pinB–H under 1.5 atm of CO_2) showed no reduction reaction after 26 h (90 °C, C_6D_6).

18. The reaction mixture was re-pressurized with 1.5 atm of CO_2 after 8 h of reaction.

19. (a) B. Wrackmeyer and O. L. Tok, *Zeitschrift für Naturforschung B*, 2006, **61**, 949–955.
(b) W. Biffar, H. Nöth, H. Pommerening and B. Wackmeyer, *Chem. Ber.*, 1980, **113**, 333–341.

20. The ^{11}B spectrum of a 1/1 **1**/pinB–H mixture (C_6D_6, RT) features a broad singlet signal at δ = 11.4 ppm significantly upfield shifted compared to that of three-coordinate pinB–H (δ 27.9 ppm), in line with a four-coordinate boron species and thus adduct formation. The ^1H NMR data are also consistent with the adduct formation, with, in particular, a upfield shift of the *Me*CO_2^- ^1H NMR resonance (δ 2.18 ppm) versus that in **1** (δ 2.39 ppm). The NMR data are all consistent with an effective C_s symmetry at RT, consistent with a fast coordination/decoordination of OAc^- on the NMR time scale. Such a fast exchange also rationalizes the non-observation of the B–*H* ^1H NMR resonance for the presumed adduct.

21. Low temperature NMR analysis of a 1/1 **1**/pinB–H mixture did not provide additional evidence on adduct formation. The putative [pinB(H)(OAc)][TBA] salt could not be isolated, perhaps due to the labile interaction between OAc^- to pinB–H.

22. The formation of a dinuclear boron species with a bridging acetate (**VI'**, ESI) is also likely and was also computed to yield slightly higher energy barriers, but could also account for the formation of formyl product **A'** (see ESI).